

# Power System Stabilizers as Undergraduate Control Design Projects

Joe H. Chow, George E. Boukarim, and Alexander Murdoch

**Abstract**—The use of power system stabilizers (PSS) to damp power system swing mode oscillations is of practical importance. The design of PSS is taught in graduate level courses on power system dynamics and control, and has been the topic of numerous M.S. and Ph.D. theses. This paper discusses the experience in assigning PSS projects in an undergraduate control design course to provide students with a challenging design problem using three different techniques and to expose them to power system engineering. The details of the PSS design projects using root-locus, frequency-domain, and state-space methods are provided.

**Index Terms**—Frequency-domain compensation, power system stabilizers, root-locus techniques, state-space methods, undergraduate design projects.

## I. INTRODUCTION

THE undergraduate level control systems engineering (CSE) course at Rensselaer Polytechnic Institute and many other universities covers the root-locus technique, frequency-response compensation, and state-space methods for control design [1]. The prerequisite of the course is the signals and systems course [2]. A course in modeling of dynamic systems [3] is helpful but not required. In the Rensselaer CSE course, the students are required to do a sequence of design projects, each corresponding to a different design technique. Past projects included a ball-and-beam system and an inverted pendulum system [4], which are challenging but tend to be more of textbook- and laboratory-type problems. To introduce the students to real-world design problems, in the Fall 2002 semester, three power system stabilizer (PSS) design problems were assigned to about 40 students. As part of the projects, the students were also required to design the voltage regulator (VR). The MATLAB package, with the Control System Toolbox and Simulink, was used for the design [5].

In assigning these problems, we needed to distill the PSS design methodologies into steps that the students could accomplish with basic design knowledge. Most of the CSE students had not taken an introductory power system analysis course, but did have notions of dynamic systems. In each project, the same single-machine, infinite-bus system model in state-space form, presented in Section II, was used. The VR was obtained first using basic design guidelines offered in textbooks [1], [6], [7]. Then with the VR loop closed, more specialized techniques were used to design the PSS to add damping to the swing mode.

In both the VR and PSS designs, realistic control specifications such as the rise time and the overshoot of step responses were given. The PSS structure and the lead-lag compensator formulas were provided to allow students to concentrate on selecting the PSS parameters. The final designs were verified by time simulation using Simulink. These design projects are described in Sections III–V. Some observations on the projects are provided in Section VI.

## II. POWER SYSTEM MODEL

A single-machine infinite-bus system (Fig. 1) was used as the design model. The machine, modeled with subtransient effects, delivers the electrical power  $P_e$  to the infinite bus. The voltage regulator controls the input  $u$  to a solid-state rectifier excitation system [8], which provides the field voltage to maintain the generator terminal voltage  $V_{term}$  at a desired value  $V_{ref}$ . The states for the machine are its rotor angle  $\delta$ , its speed  $\omega$ , and its direct- and quadrature-axis fluxes  $E'_q$ ,  $\psi_d$ ,  $E'_d$ , and  $\psi_q$ . The exciter is modeled with the voltage state  $V_R$ . All of the variables are normalized on a per-unit (p.u.) basis, except for  $\delta$  which is in radians.

The power system model is linearized at a particular equilibrium point to obtain the linearized system model given in the state-space form

$$\Delta \dot{x} = A\Delta x + B\Delta u, \quad \Delta y = C\Delta x \quad (1)$$

where  $\Delta$  denotes the perturbation of the states, input, and outputs from their equilibrium values, with

$$x = [\delta \quad \omega \quad E'_q \quad \psi_d \quad E'_d \quad \psi_q \quad V_R]^T \quad (2)$$

$$y = [V_{term} \quad \omega \quad P_e]^T. \quad (3)$$

The matrices for (1) derived from typical machine parameters are given in Appendix A. In the sequel, the  $\Delta$  symbol will be dropped to simplify notations. The dominant poles of (1) are the real pole  $s = -0.105$  associated with the field voltage response, and the electromechanical (swing) mode  $s = -0.479 \pm j9.33$  with a small damping ratio  $\zeta = 0.0513$ , representing the oscillation of machine against the infinite bus.

Starting from (1), the students were required to first use the terminal bus voltage signal  $V_{term}$  to design a high-gain VR  $K_V(s)$ . Because the VR destabilized the swing mode, a PSS  $K_d(s)$  using the machine speed signal  $\omega$  was used to add damping to the swing mode. The feedback control system block diagram implemented in Simulink is shown in Fig. 2. Note that the gain  $N$  is set to 1 for the root-locus and frequency-response designs. The input signal to a speed-input PSS is derived from

Manuscript received June 24, 2003.

J. H. Chow is with the Electrical, Computer, and Systems Engineering Department, Rensselaer Polytechnic Institute, Troy, NY 12180-3590 USA.

G. E. Boukarim and A. Murdoch are with Power System Energy Consulting Department, General Electric Company, Schenectady, NY 12345 USA.

Digital Object Identifier 10.1109/TPWRS.2003.821003

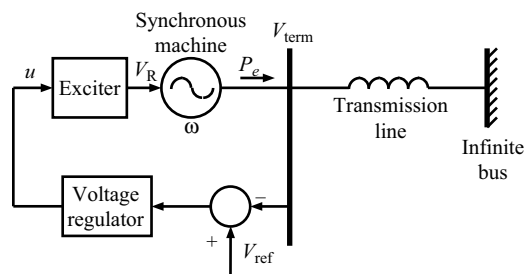


Fig. 1. Single-machine infinite-bus system.

the machine speed passed through a washout filter and several banks of torsional filters [9]. The washout (derivative) filter  $10s/(10s + 1)$  is a high-pass filter having a dc gain of 0, such that in steady state, the PSS path is not active. The aggregate phase lag effect of the torsional filters is represented by

$$G_{\text{tor}}(s) = \frac{1}{1 + 0.061s + 0.0017s^2}. \quad (4)$$

Note that the conventional PSS path comes into the  $V_{\text{ref}}$  summing junction with a positive sign. Here, we use a negative sign, balanced by a sign inversion in the feedback path, because the MATLAB root-locus function assumes negative feedback. The open- and closed-loop transfer functions required in various design stages are generated from the Simulink diagram by opening appropriate connections.

The  $P_e$  output was not used in the projects. It can be used if an instructor wants to extend the designs to a dual-input PSS with both the machine speed and the output power as the input signals [10]–[12].

Detailed discussions of PSS design techniques based on the synchronizing and damping torque concept can be found in many excellent references such as [13]–[15]. In the PSS projects, these ideas were translated into procedures that could be followed by students with basic control system design skills.

### III. ROOT-LOCUS DESIGN

#### A. Design Tasks

The first project in the sequence was the design of the VR and the PSS using root-locus techniques, which are usually taught first in a control systems course. The process was specified in several tasks:

- (R1) For a 0.1-p.u. step in  $V_{\text{ref}}$ , simulate the  $V_{\text{term}}$  response of the open-loop system (1) up to 10 s. Then with the PSS-loop open, repeat the simulation for (1) controlled by a proportional VR  $K_V(s) = K_p$  with  $K_p = 10, 20, \dots, 50$ .
- (R2) Make a root-locus plot of the voltage regulation loop using the proportional controller and find the gain  $K_u$  when the lightly damped swing mode becomes unstable.
- (R3) Apply a PI controller for the VR

$$K_V(s) = K_{\text{PI}}(s) = K_p \left( 1 + \frac{K_I}{s} \right) \quad (5)$$

and plot the closed-loop  $V_{\text{term}}$  response to a 0.1-p.u.  $V_{\text{ref}}$  step input. Select the parameters from  $0 < K_p <$

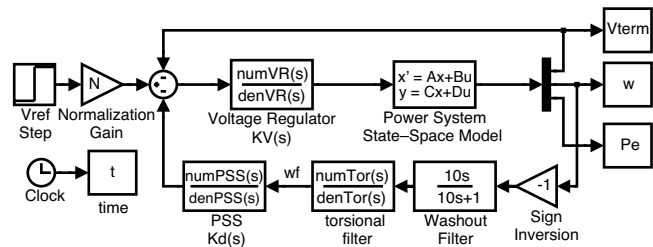


Fig. 2. Control structure of the single-machine infinite-bus system.

$K_u$  and  $0.1 < K_I < 10$  such that the rise time  $t_r$  is less than 0.5 s and the overshoot  $M_p$  is about 10%. These specifications reflect the requirements of modern high-gain VRs.

- (R4) Close the voltage regulation loop with  $K_{\text{PI}}(s)$  and perform a root-locus analysis of the PSS loop using the transfer function from  $V_{\text{ref}}$  to  $\omega_f$ , the output of the torsional filter, assuming  $K_d(s)$  to be a proportional gain control. Find the angle of departure  $\phi_{\text{dep}}$  of the root-locus branch leaving the swing mode with the positive imaginary part.
- (R5) Based on  $\phi_{\text{dep}}$ , design a second-order phase-lead compensator

$$K_d(s) = K_{\text{Id}} \left[ \alpha_{\text{Id}1} \frac{s - z_{\text{Id}1}}{s - p_{\text{Id}1}} \right] \left[ \alpha_{\text{Id}2} \frac{s - z_{\text{Id}2}}{s - p_{\text{Id}2}} \right] \quad (6)$$

$$p_{\text{Id}i} = \alpha_{\text{Id}i} z_{\text{Id}i}, \quad \alpha_{\text{Id}i} > 1, \quad i = 1, 2 \quad (7)$$

using the phase-lead properties described in Appendix B, such that the angle of departure of the compensated system is about  $180^\circ$ . Perform another root-locus analysis for (6) and select  $K_{\text{Id}}$  to achieve a damping ratio  $\zeta \geq 15\%$  for the swing mode.

- (R6) Implement  $K_d(s)$  in the Simulink diagram and simulate the closed-loop  $V_{\text{term}}$  response to a 0.1-p.u.  $V_{\text{ref}}$  step input. Check if  $t_r \leq 0.5$  s and  $M_p \leq 10\%$  have been satisfied.

#### B. Discussion of Design

Tasks R1 and R2 reveal important properties of the system and the proportional control. Fig. 3 shows the open-loop step response and the responses for the different  $K_p$  values. Note the slow open-loop response which settles to 0.0747 p.u., yielding a 25% steady-state error. As  $K_p$  increases, the closed-loop step response becomes faster and the steady-state error smaller, but the oscillation due to the swing mode becomes less damped. At  $K_p = 50$ , the feedback system is unstable with a growing oscillation. The instability can be studied with a root-locus plot, as shown in Fig. 4. As  $K_p$  increases, the voltage mode moves left from  $s = -0.105$ , thus improving  $t_r$ . The swing mode, however, is destabilized, and crosses the imaginary axis at  $K_u \approx 47$ . Although the system becomes stable again as  $K_p$  is increased beyond 1260, such a high gain is nonrobust because any reduction in the system gain due to changing operating condition would pull the swing mode back into the right half-plane. Thus, the proportional gain has to be kept below 47.

A good way to approach task R3 is to set up a grid of  $K_p$  and  $K_I$  values and simulate the step response by sweeping through

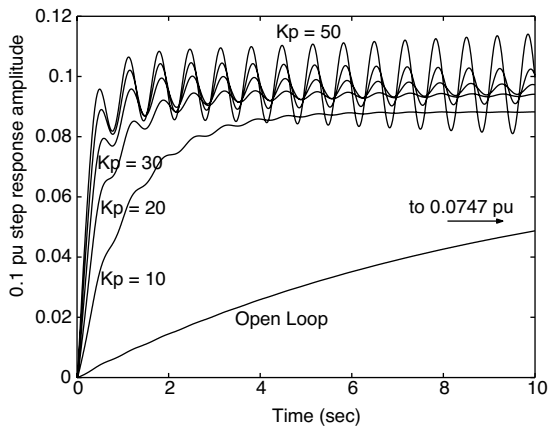


Fig. 3.  $V_{term}$  responses to step in  $V_{ref}$ , open loop, and closed loop for  $K_p = 10, 20, \dots, 50$ .

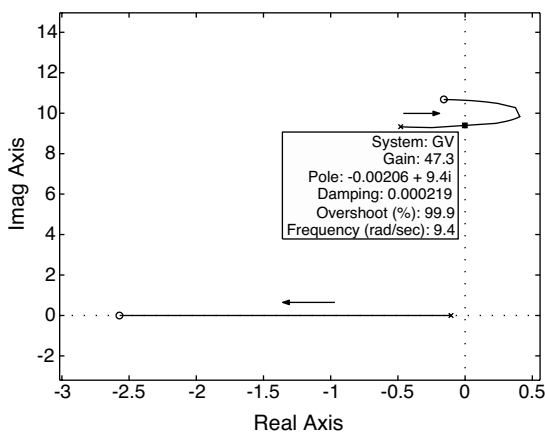


Fig. 4. Root-locus plot of voltage regulation loop.

the grid values. Note that new commercial digital VRs have integral actions, although older analog VRs usually have a high proportional gain for tighter steady-state regulation and a lag-lead block for transient gain reduction. One set of values that will satisfy the design specifications is  $K_p = 35$  and  $K_I = 0.4$ , whose step response is shown as the dashed curve in Fig. 5, with  $t_r = 0.446$  s and  $M_p = 12.5\%$ . The integral action has removed the steady-state error. We leave some margin in  $t_r$  because a PSS will slow down the time response. On the other hand, with a PSS providing additional damping, the overshoot will be reduced.

In task R4, we close the VR loop and add in the washout filter and  $G_{tor}(s)$  to generate the transfer function from  $V_{ref}$  to the PSS input. Taking the PSS to be a proportional controller, the departure angle of the root-locus branch leaving the swing mode is about  $60^\circ$  (Fig. 6). To add purely damping to the swing mode, the departure angle should be  $180^\circ$ . Thus, for task R5, we need to add a  $120^\circ$  compensation at the swing-mode frequency in the feedback loop using a phase-lead controller. From Fig. 17, this  $120^\circ$  compensation requires two first-order phase-lead compensators in series. Setting the two compensators to be identical, we obtain  $\alpha_{ld} = 14$ , with the swing mode frequency of 9.33 rad/s as the center frequency  $\omega_c$ . The root-locus analysis is repeated with the phase compensation in the feedback loop. Fig. 7 shows the swing mode having a departure angle close to  $180^\circ$ , allowing

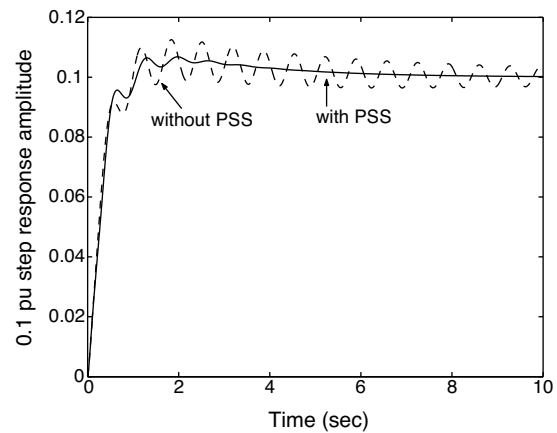


Fig. 5.  $V_{term}$  responses to step in  $V_{ref}$  with  $K_{PI}(s)$  (5).

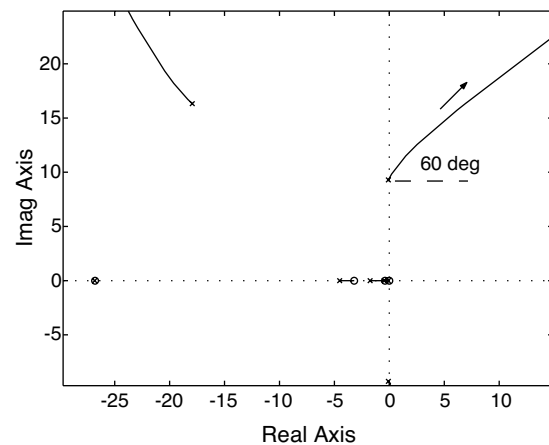


Fig. 6. Root-locus plot of swing mode using proportional gain PSS.

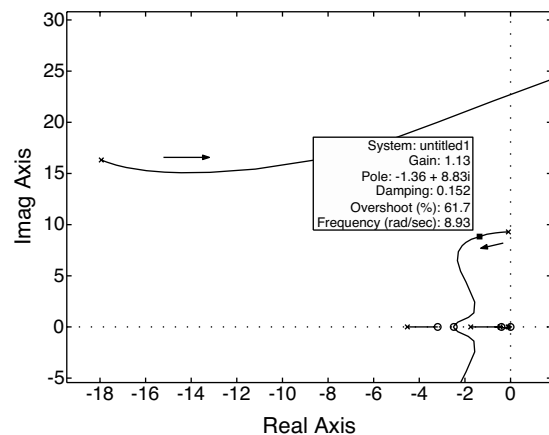


Fig. 7. Root-locus plot of swing mode with PSS (8).

the selection of the PSS gain at 1.13 to achieve a 15% damping ratio. The PSS thus has the form

$$K_d(s) = 1.13 \left[ \frac{14(s + 2.94)}{s + 34.9} \right]^2. \quad (8)$$

When the PSS loop is closed, the  $V_{term}$  response to a 0.1-p.u. step in  $V_{ref}$ , shown as the solid curve in Fig. 5, has  $t_r = 0.456$  s and  $M_p = 6.81\%$ , satisfying the design specifications.

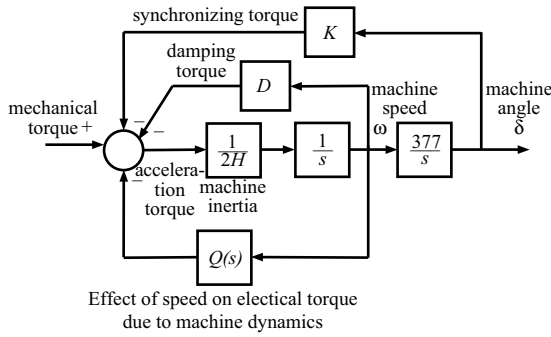


Fig. 8. Decomposition of speed control loop.

#### IV. FREQUENCY-RESPONSE DESIGN

##### A. Design Tasks

The second project required the use of frequency-response design techniques. The VR design was quite standard, whereas the PSS design required decomposing the accelerating torque on the synchronous machine into its synchronizing and damping components. To guide the design process, the following tasks were specified.

- (F1) Plot the frequency response of the system from  $u$  to  $V_{\text{term}}$ . Find the dc gain and the gain and phase margins of the uncompensated system.
- (F2) Design a phase-lag controller  $K_V(s)$

$$K_V(s) = K_{\text{lg}} \frac{s - z_{\text{lg}}}{s - p_{\text{lg}}} \quad (9)$$

such that the dc gain of the compensated system is at least 200 and the phase margin is at least  $80^\circ$ . Plot the compensated system frequency response and find the gain and phase margins.

- (F3) Close the voltage regulation loop and simulate the  $V_{\text{term}}$  response of the closed-loop system to a 0.1-p.u.  $V_{\text{ref}}$  step input. Find  $t_r$ ,  $M_p$ , and the steady-state error.
- (F4) Generate the state-space model  $G_\omega(s)$  from  $V_{\text{ref}}$  to  $\omega$  with the lag controller  $K_V(s)$  loop closed. Regarding the power system model as a second-order mass-spring system, decompose the model to isolate the  $Q(s)$  path from the speed to the electrical torque, as shown in Fig. 8. The resulting system  $A_\omega$  matrix has the structure

$$A_\omega = \begin{bmatrix} 0 & 376.99 & 0 \\ -K & -D & a_{23} \\ a_{31} & a_{32} & A_{33} \end{bmatrix} \quad (10)$$

where  $K = 0.2462$ ,  $D = 0.1563$ ,  $a_{23}$  is a row vector,  $a_{31}$  and  $a_{32}$  are column vectors, and  $A_{33}$  is a square matrix. Construct the state-space model  $Q(s)$  with the machine speed  $\omega$  as the input and the electrical torque  $\tau$  as the output

$$\dot{\xi} = A_{33}\xi + a_{32}\omega, \quad \tau = a_{23}\xi. \quad (11)$$

Connect  $Q(s)$  in series with the washout and torsional filters to form  $F(s)$ . Plot the frequency response of  $F(s)$ , using a frequency range of 1 to 100 rad/s.

- (F5) Design a phase-lead controller  $K_d(s)$  (6) such that the phase of  $F(s)K_d(s)$  is between  $0$  to  $-20^\circ$  from 2 to 12 rad/s (approximately 0.3 to 2 Hz). The rationale is that if the phase of  $F(s)K_d(s)$  is close to zero and slightly negative, the speed feedback loop will add mostly damping. Furthermore, the root-locus departure angle from the swing mode will be slightly less than  $180^\circ$ , such that the swing mode frequency will increase, improving the synchronizing torque. By specifying a frequency range, improved damping is possible whenever the swing frequency, which can change according to the operating condition, falls in this range. Again, the phase-lead compensator characteristics in Appendix B will be helpful. For the designed  $K_d(s)$ , plot the frequency response of  $F(s)K_d(s)$  with  $K_{\text{ld}} = 1$ .
- (F6) Connect  $G_\omega(s)$  in series with  $K_d(s)$ , the washout filter, and  $G_{\text{tor}}(s)$ . Use this system to perform a root-locus analysis to select  $K_{\text{ld}}$  to achieve a damping ratio  $\zeta = 15\%$  for the swing mode.
- (F7) Implement  $K_d(s)$  in the Simulink diagram and simulate the  $V_{\text{term}}$  response due to a 0.1-p.u.  $V_{\text{ref}}$  step input. Find  $t_r$ ,  $M_p$ , and the steady-state error.
- (F8) As a final check, in the Simulink diagram, disconnect the feedback path from  $V_R(s)$  into the input summing junction, and generate the linear model from  $V_{\text{ref}}$  to the output of  $V_R(s)$  with the  $K_d(s)$  loop closed. Find the gain and phase margins of the compensated system.

##### B. Discussion of Design

The uncompensated system frequency response plot in Fig. 9 shows that the magnitude of the open-loop system is less than unity, with the dc gain at 0.747 and a local magnitude peak at  $\omega = 9.33$  rad/s due to the lightly damped swing mode. This swing mode also determines the gain margin to be 33 dB (44.67). We set the high-frequency gain  $K_{\text{lg}}$  of  $K_V(s)$  at 40, so that the new gain-crossover frequency  $\omega_{\text{gc}}$  of the compensated system is about 3.6 rad/s, with a phase of about  $-90^\circ$ . Using the phase-lag design procedure in [1, p. 405], we set the controller low-frequency gain, the zero, and the pole to be

$$K_{\text{LF}} = \frac{200}{0.747 K_{\text{lg}}} \quad (12)$$

$$z_{\text{lg}} = -\frac{\omega_{\text{gc}}}{10}, \quad p_{\text{lg}} = -\frac{z_{\text{lg}}}{K_{\text{LF}}} \quad (13)$$

such that

$$K_V(s) = 40 \frac{s + 0.36}{s + 0.0538}. \quad (14)$$

The frequency-response plot of the compensated system is also shown in Fig. 9, indicating a low-frequency gain of 200 and a phase margin of  $85.5^\circ$ . Due to the local magnitude peak of the swing mode, the gain margin is only 0.85 dB, which will be improved by the PSS. The closed-loop system response to a 0.1-p.u. step in  $V_{\text{ref}}$  is shown as the dashed curve in Fig. 10, with  $t_r = 0.414$  s and  $M_p = 11.4\%$ .

In task F4, we construct  $F(s)$  and plot its frequency response in Fig. 11. Note that the phase of  $F(s)$  is  $-40.3^\circ$  at 2 rad/s

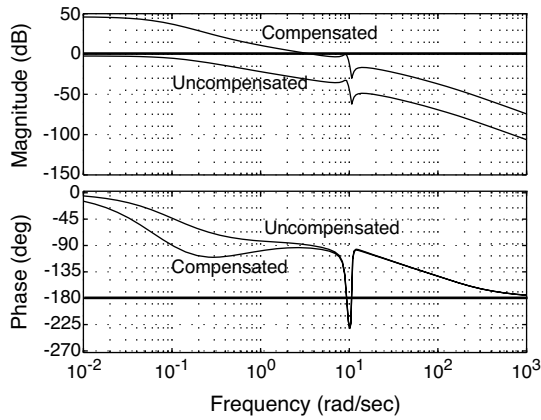
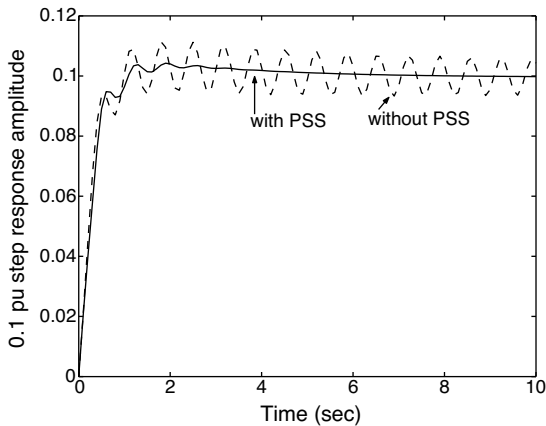


Fig. 9. Frequency responses of voltage regulation loop.

Fig. 10.  $V_{\text{term}}$  responses to step in  $V_{\text{ref}}$  with lag controller (14).

and drops to  $-133^\circ$  at 12 rad/s. According to the phase specifications, we need to add at least  $113^\circ$  at 12 rad/s. The center frequency of the desired lead controller will be higher than the value of 9.33 rad/s used in (8). After a few design iterations, the values  $\omega_{1d} = 13.7$  and  $\omega_c = 20$  rad/s are selected for both lead stages. To set the gain, we perform a root-locus analysis, as shown in Fig. 12, obtaining a gain of 3.75 to achieve a 15% damping ratio of the swing mode. Thus, the PSS has the form

$$K_d(s) = 3.75 \left[ \frac{13.7(s + 5.40)}{s + 74.0} \right]^2. \quad (15)$$

When the PSS loop is closed, the system response to a 0.1-p.u. step in  $V_{\text{ref}}$  is shown as the solid curve in Fig. 10. Note that in this response,  $t_r = 0.468$  s and  $M_p = 4.24\%$ , which are similar to those obtained from the root-locus design.

In task F8, with the PSS adding damping and reducing the local magnitude peak due to the swing mode, the gain margin in the voltage loop improves to 10 dB.

## V. STATE-SPACE DESIGN

### A. Design Tasks

In the third project, full-state feedback laws and observers derived from pole placement were used to design and implement

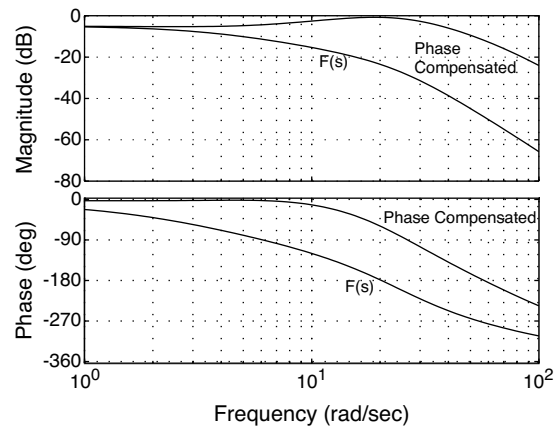
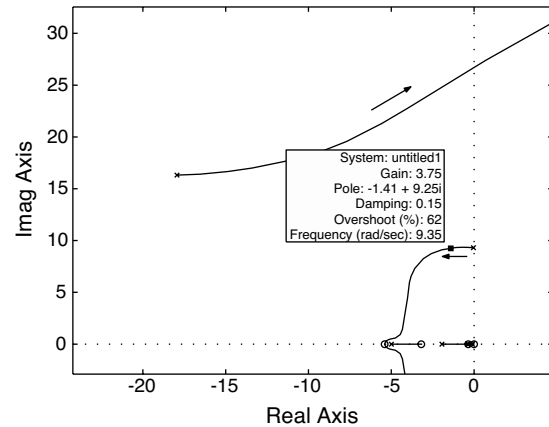
Fig. 11. Frequency responses of  $F(s)$  and  $F(s)K_d(s)$ .

Fig. 12. Root-locus plot of swing mode for (15).

the VR and PSS [16]. State-space design is not commonly used for PSS design because the controller order may be high. Thus, in this project, it was essential that some model reduction steps be taken to obtain low-order controllers. The design tasks were as follows:

- (S1) With the PSS-loop open, use  $u$  as the input and  $V_{\text{term}}$  as the output, to obtain a single-input, single-output model. Design a full-state feedback control to place the closed-loop voltage regulation pole at the desired location to reduce the voltage control time constant, leaving all of the other poles unchanged. Then, design an observer so that the system states can be estimated from  $V_{\text{term}}$  by ensuring that the voltage control transient due to the observer pole decays faster than the full-state feedback pole. Implement the observer-based controller  $K_{V_o}(s)$  and the scalar gain  $N$  such that for a 0.1-p.u. step input  $V_{\text{ref}}$ , the closed-loop  $V_{\text{term}}$  response achieves  $t_r < 0.5$  s,  $M_p < 5\%$ , and zero steady-state voltage regulation error.
- (S2) The controller  $K_{V_o}(s)$  obtained from task S1 is seventh order, with much of its dynamics not important. In this task, we will preserve only its voltage regulation function. First, plot the frequency response of  $K_{V_o}(s)$ . Then, express  $K_{V_o}(s)$  in the zero-pole-gain form and

perform approximate pole-zero cancellations to retain only a first-order reduced controller  $K_V(s)$

$$K_V(s) = \frac{K_p}{s - p_d} \quad (16)$$

where  $K_p$  is selected so that  $K_V(s)$  and  $K_{V_o}(s)$  have the same dc gain. Plot the frequency response of  $K_V(s)$  versus that of  $K_{V_o}(s)$ . Close the voltage loop with  $K_V(s)$  and perform a step response with a 0.1-p.u.  $V_{\text{ref}}$  step input. Compare it to the step response using  $K_{V_o}(s)$ .

- (S3) Generate the state-space model  $G_\omega(s)$  from  $V_{\text{ref}}$  to  $\omega_f$  with  $K_V(s)$  (16) implemented. The controller  $K_{do}(s)$  is designed to improve the damping ratio of the swing mode to 15% by first obtaining a full-state feedback control to add damping to the swing mode and then an observer so that the states of the system can be estimated using  $\omega_f$ . Construct the 11th-order observer-based controller  $K_{do}(s)$ , which also has some dynamics that are not important. Apply the minimal realization function `minreal` in the MATLAB Control System Toolbox to obtain a controller  $K_d(s)$ . Do a root-locus analysis of the damping controller loop using  $K_d(s)$ . Close the damping control loop with  $K_d(s)$  and simulate the  $V_{\text{term}}$  response of the overall closed-loop system to a 0.1-p.u.  $V_{\text{ref}}$  step input. Find  $t_r$  and  $M_p$ .

### B. Discussion of Design

Because the open-loop voltage pole is at  $s = -0.105$ , it is essential that this pole be made faster in order to improve the voltage response. In task S1, this pole will be shifted to  $s = -4$  for the full-state feedback design and to  $s = -8$  in the observer design. The resulting seventh-order  $K_{V_o}(s)$  is given in Table I, whose frequency response is shown in Fig. 13. For zero steady-state voltage error, we set  $N = 1.037$ . The closed-loop response to a 0.1-p.u. step in  $V_{\text{ref}}$  shown as the dot-dashed plot in Fig. 14 processes only a small amount of oscillations, with  $t_r = 0.433$  s and  $M_p = 4.6\%$ . The frequency response of  $K_{V_o}(s)$  exhibits a notch filter characteristic at the swing mode, reducing its effect on the swing mode. This design strategy is not robust, because the swing frequency can vary with the operating condition.

Table I shows that the zeros and poles form approximate pairs except for the pole at  $s = -13.19$ . This pole will be retained in (16) such that

$$K_V(s) = \frac{483.5}{s + 13.19} \quad (17)$$

whose frequency response no longer has a notch filter characteristic, as shown in Fig. 13. Thus, the time response of the closed-loop system, shown as the dashed plot in Fig. 14, is oscillatory.

In task S3 for the full-state feedback design, the swing mode is shifted to  $-1.5 \pm j9.06$  to achieve a slightly higher than 15% damping ratio, and for the observer design, the swing mode is shifted to  $-4.5 \pm j9.06$  to ensure fast tracking. All of the other poles are fixed. The frequency response of the 11th-order ob-

TABLE I  
ZEROS, POLES, AND GAIN OF  $K_{V_o}(s)$

zeros	-114.7, -35.4, -26.8, -3.08, $-0.479 \pm j9.33$
poles	-114.6, -34.6, -26.8, -13.19, $-2.243, -0.609 \pm j9.50$
gain	392.6

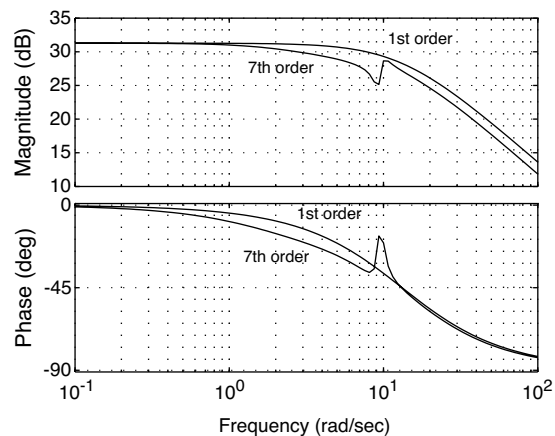


Fig. 13. Frequency responses of  $K_{V_o}(s)$  and  $K_V(s)$ .

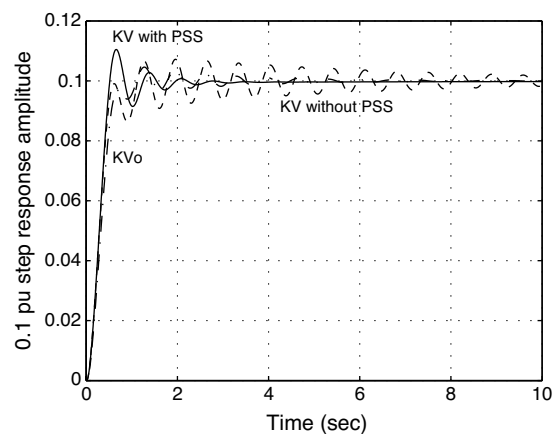


Fig. 14.  $V_{\text{term}}$  responses to step in  $V_{\text{ref}}$  for  $K_{V_o}(s)$  and  $K_V(s)$ .

server-based controller  $K_{do}(s)$  is shown in Fig. 15. Note the phase-lead characteristic of  $K_{do}(s)$ . Using the `minreal` function with a tolerance of 0.001, a fifth-order controller  $K_d(s)$  is obtained. Fig. 15 shows that the frequency responses of  $K_{do}(s)$  and  $K_d(s)$  match closely.

An interesting aspect of the state-space design is that in the root-locus plot using  $K_d(s)$ , the root-locus branch (Fig. 16) moves from the swing mode almost parallel to the negative real axis, providing purely damping enhancement. When the PSS loop is closed, the  $V_{\text{term}}$  response to a 0.1-p.u. step in  $V_{\text{ref}}$  is shown as the solid curve in Fig. 14. Note that this response has a fast rise time  $t_r = 0.350$  s, but a higher overshoot  $M_p = 10.5\%$ .

## VI. PEDAGOGY

In a typical undergraduate control systems course, each of the three design techniques are covered in about three weeks. At Rensselaer, these design projects were assigned concurrently with their lecture discussions. One lecture was spent on a detailed discussion of each design project. Students were allowed

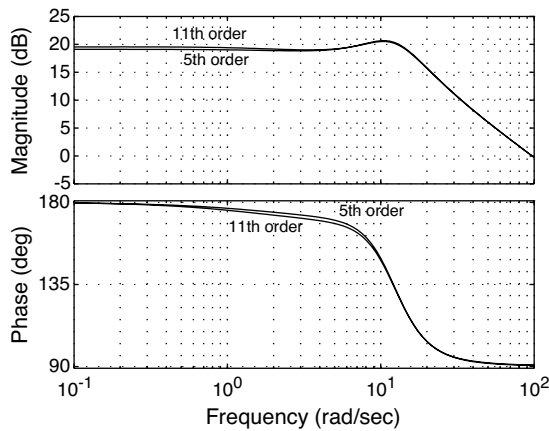


Fig. 15. Frequency responses of  $K_{do}(s)$  and  $K_d(s)$ .

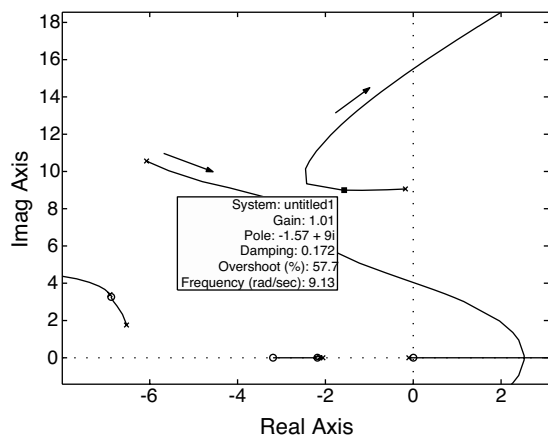


Fig. 16. Root-locus plot of swing mode using  $K_d(s)$ .

to form two-person teams and had about two to three weeks to complete each project.

Feedback and closed-loop systems are among the hardest concepts for many engineering students to have a good grasp. Good design projects with powerful simulation tools can be very helpful in reinforcing theoretical analysis. In addition, applying different techniques to the same design problem provides insights into the linkage of the design concepts. Many students were amazed at how well their VRs and PSSs performed, and the design experience became a favorite discussion topic in their job interviews. Many students also included these design projects on their resués.

In the design projects, we provided a Simulink diagram for the students to implement the controllers, considering that the design required closing two single-input, single-output loops, one for regulation and the other for stabilization. Although the projects could be accomplished solely using the MATLAB command language, operations with Simulink diagram removed most of the drudgery of keeping track of the feedback structure, reducing the possibility of errors. This was an important consideration when most of the students were not proficient MATLAB users before taking this control systems course.

Toward the end of the semester, one of the co-authors (GEB) of this paper gave a lecture to the students on PSS design tools

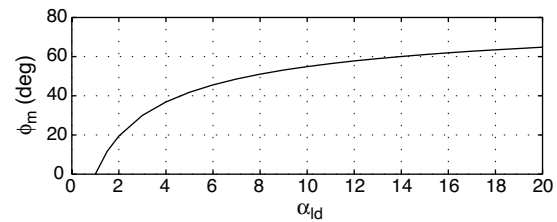


Fig. 17. Maximum phase angle  $\phi_m$  versus  $\alpha_{ld}$ .

used in industry and PSS tuning during commissioning. Although such industry interactions can be readily arranged at Rensselaer because of her proximity to a turbine-generator manufacturer, with advance planning, it is possible for other schools to do likewise.

## VII. CONCLUSION

In this paper, we have presented three PSS design projects, based on the root-locus, frequency-response, and state-space methods, for an undergraduate control systems course. The projects provided students with some realistic and challenging design experience and exposed them to a well-known power system design problem. The course survey indicated that the students were generally pleased with the design activities.

Any one of the PSS design projects can be adopted for use with modifications by instructors of similar courses. A saturation block can be added to the output of the PSS to limit its contribution in the voltage regulator input. The design specifications can be either relaxed or tightened. For a graduate-level design course, a PSS design for multiple-machine systems or the dual-input PSS design can be addressed. In addition, PSS designs for systems with multiple operating conditions can be considered. More advanced techniques such as fuzzy logic [17] and genetic algorithms [18] can also be applied, depending on the needs of the course.

## APPENDIX

### VIII. STATE-SPACE MODEL

The matrices for the state-space model (1) are shown in the equation at the bottom of the top page.

The system data can also be downloaded from the web site [www.brookscole.com](http://www.brookscole.com), which provides resources for the text [4].

### IX. PHASE-LEAD COMPENSATION

The single-stage phase-lead controller

$$G(s) = \alpha_{ld} \frac{s - z_{ld}}{s - p_{ld}}, \quad p_{ld} = \alpha_{ld} z_{ld}, \quad \alpha_{ld} > 1 \quad (18)$$

has its zero  $s = z_{ld}$  closer to the origin of the  $s$ -plane than its pole  $s = p_{ld}$ . At low frequencies, its gain is unity and its phase is zero. At high frequencies, its gain is  $\alpha_{ld}$  and its phase is zero. At the center frequency defined as  $\omega_c = \sqrt{z_{ld} p_{ld}}$ , it has the maximum phase lead of

$$\sin \phi_m = \frac{\alpha_{ld} - 1}{\alpha_{ld} + 1}. \quad (19)$$

$$A = \begin{bmatrix} 0 & 377.0 & 0 & 0 & 0 & 0 & 0 \\ -0.246 & -0.156 & -0.137 & -0.123 & -0.0124 & -0.0546 & 0 \\ 0.109 & 0.262 & -2.17 & 2.30 & -0.0171 & -0.0753 & 1.27 \\ -4.58 & 0 & 30.0 & -34.3 & 0 & 0 & 0 \\ -0.161 & 0 & 0 & 0 & -8.44 & 6.33 & 0 \\ -1.70 & 0 & 0 & 0 & 15.2 & -21.5 & 0 \\ -33.9 & -23.1 & 6.86 & -59.5 & 1.50 & 6.63 & -114 \end{bmatrix}$$

$$B = [0 \ 0 \ 0 \ 0 \ 0 \ 0 \ 16.4]^T$$

$$C = \begin{bmatrix} -0.123 & 1.05 & 0.230 & 0.207 & -0.105 & -0.460 & 0 \\ 0 & 1 & 0 & 0 & 0 & 0 & 0 \\ 1.42 & 0.900 & 0.787 & 0.708 & 0.0713 & 0.314 & 0 \end{bmatrix}.$$

Fig. 17 shows  $\phi_m$  as a function of  $\alpha_{fd}$ , which is useful for selecting the appropriate  $\alpha_{fd}$  to achieve a desired phase lead [6].

#### REFERENCES

- [1] G. F. Franklin, J. D. Powell, and A. Emami-Naeini, *Feedback Control of Dynamic Systems*, 4th ed. Reading, MA: Addison-Wesley, 2002.
- [2] A. V. Oppenheim and A. S. Willsky, *Signals and Systems*, 2nd ed. Englewood Cliffs, NJ: Prentice-Hall, 1997.
- [3] C. M. Close, D. K. Frederick, and J. Newell, *Modeling and Analysis of Dynamic Systems*, 3rd ed. New York: Wiley, 2002.
- [4] D. K. Frederick and J. H. Chow, *Feedback Control Problems using MATLAB and the Control System Toolbox*: Brooks/Cole, 2000.
- [5] The MathWorks, Inc., *Using MATLAB and Using Simulink*, 2002.
- [6] R. C. Dorf and R. H. Bishop, *Modern Control Systems*, 9th ed. Reading, MA: Addison-Wesley, 2001, p. 559.
- [7] B. C. Kuo and M. F. Golnaraghi, *Automatic Control Systems*, 8th ed. New York: Wiley, 2003.
- [8] P. Kundur, *Power System Stability and Control*. New York: McGraw-Hill, 1994.
- [9] R. A. Lawson, D. A. Swann, and G. F. Wright, "Minimization of power system stabilizer torsional interaction on large steam turbine-generators," *IEEE Trans. Power App. Syst.*, vol. PAS-97, pp. 183–190, Jan./Feb. 1978.
- [10] Digital Excitation System Task Force of the Equipment Working Group, "Computer models for representation of digital-based excitation systems," *IEEE Trans. Energy Conversion*, vol. 11, pp. 607–615, Sept. 1996.
- [11] A. Murdoch, S. Venkataraman, R. A. Lawson, and W. R. Pearson, "Integral of accelerating power type PSS—Part 1—theory, design, and tuning methodology," *IEEE Trans. Energy Conversion*, vol. 14, pp. 1658–1663, Dec. 1999.
- [12] A. Murdoch, S. Venkataraman, and R. A. Lawson, "Integral of accelerating power type PSS—Part 2—field testing and performance verification," *IEEE Trans. Energy Conversion*, vol. 14, pp. 1664–1672, Dec. 1999.
- [13] F. P. deMello and C. Concordia, "Concept of synchronous machine stability as affected by excitation control," *IEEE Trans. Power App. Syst.*, vol. PAS-88, pp. 189–202, Apr. 1969.
- [14] E. V. Larsen and D. A. Swann, "Applying power system stabilizers, parts I–III," *IEEE Trans. Power App. Syst.*, vol. PAS-100, pp. 3017–3046, June 1981.
- [15] P. Kundur, M. Klein, G. J. Rogers, and M. S. Zywno, "Application of power system stabilizers for enhancement of overall system stability," *IEEE Trans. Power Syst.*, vol. PWR-4, pp. 614–626, May 1989.
- [16] J. H. Chow and J. J. Sanchez-Gasca, "Pole-placement designs of power system stabilizers," *IEEE Trans. Power Syst.*, vol. 4, pp. 271–277, Feb. 1989.
- [17] T. Hiyama, "Robustness of fuzzy logic power system stabilizers applied to multimachine power system," *IEEE Trans. Energy Conversion*, vol. 9, pp. 451–459, Sept. 1994.
- [18] A. L. B. Do Bomfim, G. N. Taranto, and D. M. Falcao, "Simultaneous tuning of power system damping controllers using genetic algorithms," *IEEE Trans. Power Syst.*, vol. 15, pp. 163–169, Feb. 2000.

**Joe H. Chow** received the B.S.E.E. and B.Math degrees from the University of Minnesota, Minneapolis, and the M.S. and Ph.D. degrees from the University of Illinois at Urbana-Champaign.

Currently, he is Professor of Electrical, Computer, and Systems Engineering at Rensselaer Polytechnic Institute (RPI), Troy, NY. Before joining RPI, he worked in the power system division of General Electric Company, Schenectady, NY. His research interests include modeling and control of power systems.

**George E. Boukarim** received the B.S., M.E., and Ph.D. degrees in electric power engineering from Rensselaer Polytechnic Institute, Troy, NY, in 1987, 1988, and 1998, respectively.

From 1988 to 1994 and from 1998 to the present he was with the Power Systems Energy Consulting (PSEC) Department of the General Electric Company, Schenectady, NY, working in the area of power system dynamics and control. He also worked for the Transmission Technology Institute, Schenectady, NY, ABB Power T&D Company, Raleigh, NC, for a short period from 1997 to 1998. His interests include robust multivariable control, and power system dynamics and control.

**Alexander Murdoch** received the B.S.E.E. degree from Worcester Polytechnic Institute, Worcester, MA, in 1970, and the M.S.E.E. and Ph.D. degrees from Purdue University, West Lafayette, IN, in 1972 and 1975, respectively.

Currently, he is a Consulting Engineer with General Electric, working in Power Systems Energy Consulting (PSEC), Schenectady, NY. He joined General Electric in 1975 and has worked primarily at PSEC but also for Drive System, Salem, VA. His areas of interest include rotating machine modeling, excitation system design and testing, and advanced control theory.

Dr. Murdoch is a member of the Excitation System Subcommittee in the IEEE.